Glass-Transition Cooperativity Onset in a Series of Random Copolymers Poly(*n*-butyl methacrylate-*stat*-styrene)

S. Kahle,[†] J. Korus,[†] E. Hempel,[†] R. Unger,[†] S. Höring,[‡] K. Schröter,[†] and E. Donth*,[†]

Fachbereich Physik and Fachbereich Chemie, Universität Halle, D-06099 Halle (Saale), Germany

Received December 31, 1996; Revised Manuscript Received August 6, 1997[⊗]

ABSTRACT: Dielectric spectroscopy, heat capacity spectroscopy (HCS), and differential scanning calorimetry (DSC) investigations in the $\alpha\beta$ relaxation splitting region of a series of random copolymers of *n*-butyl methacrylate with styrene are reported. A separate onset of the α relaxation is dielectrically observed, about one frequency decade below a continuous local $a\beta$ component in the Arrhenius diagram. This splitting scenario shifts to higher frequencies and temperatures for increasing styrene content and does not qualitatively change from homo PnBMA up to 54 mol % styrene. The logarithms of onset frequency, log ω_{on}, and of WLF asymptotic frequency, log Ω, change linearly with the styrene content, but their ratio is constant and remains large, $\log_{10}(\Omega/\omega_{on}) = 3.8 \pm 1$. The log $\Omega \approx 7$ (rad/s) values for small styrene content are unusually low. Ω is explained as the frequency of local cooperativity chances in the concept of kinetic molecular randomness for the dynamic glass transition. The α dielectric intensity, $\Delta\epsilon_\alpha$, the caloric intensity, Δc_p, and the square root of cooperativity from a fluctuation formula, $N_\alpha^{1/2}$, are linearly proportional to the temperature difference to the onset, e.g. $\Delta\epsilon_\alpha \sim (T_{on} - T)$. The dielectric activities of the α process and a hypothetical γ process (beyond the Johari Goldstein β process) increase with increasing styrene content although the styrene unit is almost nonpolar. This is interpreted by dipole decompensation for the α and γ relaxation modes caused by the random styrene units.

I. Introduction

The size of glass-transition cooperativity has been an ongoing issue.[1−4] Experimental evidences of an onset of this cooperativity would be of particular interest, because such a complex phenomenon as molecular cooperativity can surely better be understood when its origin, and its increase below the origin, is accessible to experimental studies.

The present experimental situation for such a cooperativity onset can be characterized by three aspects.

The first is that when a glass-forming molecular liquid is cooled down from high temperatures, far below the terahertz $\alpha\beta_{fast}$ splitting temperature[5,6] a further anomaly is regularly observed along the α dispersion zone = dynamic glass transition: the $\alpha\beta$ (Johari Goldstein) splitting, or a region where the Stokes−Einstein−Debye relation becomes violated,[7] or a dielectric peculiarity, e.g. the T_A temperature of Fischer.[8] It was suggested[8,9] that this anomaly be connected with an α onset temperature T_{on} (compliance step $\Delta\chi_\alpha \rightarrow 0$ in linear extrapolation[10]) of a typical glass-transition cooperativity in the sense of Adam and Gibbs.[1] Usually, the corresponding onset frequency ω_{on} is in the mega- to gigahertz range and, therefore, not so easily accessible by linear response experiments, e.g., by shear and heat capacity spectroscopy HCS.

The second is that when the alkyl group in a series of poly(*n*-alkyl methacrylates), including a series of random copolymers of the propyl and pentyl members, is enlarged, the $\alpha\beta$ splitting region containing some kind of an α onset is systematically shifted to lower frequency ranges that are commonly accessible by dielectric (ϵ^*), HCS (c_p^*), and shear linear response methods.[10,11] The onset character is indicated by a steep linear increase of dielectric α relaxation intensities, starting from zero, $\Delta\epsilon_\alpha \sim (T_{on} - T)$, which is observed in many samples of this series. Besides the onset temperature T_{on}, the onset is characterized by an onset frequency, ω_{on}, determined from the α relaxation trace of the dielectric loss maximum below the onset by means of a VFT[12] equation

$$\log \omega = \log \Omega - B/(T - T_\infty) \qquad (1)$$

with the interesting property that the Ω/ω_{on} ratio is large, e.g. $\log(\Omega/\omega_{on}) \equiv \log_{10}(\Omega/\omega_{on}) \approx 4$. The onset is far below the frequency asymptote Ω for the α relaxation.

The relation of eq 1 to the usual notation of WLF,[13] $\log(\omega/\omega_0) = -c_1^0(T - T_0)/(c_2^0 + T - T_0)$, is $c_1^0 = \log(\Omega/\omega_0)$,[9] $c_2^0 = T_0 - T_\infty$, and $B = c_1^0 c_2^0$; T_∞ is the Vogel temperature.

The third aspect is that, in the $\alpha\beta$ splitting region, different activities can now be observed.[14,15] Whereas dielectric and shear response are sensitive to both relaxations, α and β, the calorimetric HCS activity is only sensitive (i.e. $\Delta c_p/\overline{c_p}$ larger than a few percent) to the α relaxation. Since the calorimetric factor (c_p^*) of the HCS signal can be interpreted as an entropy compliance,[9] it has been suggested to connect this entropy activity with cooperativity. This means, that α is cooperative, and β is not. A cooperativity onset is, therefore, expected to be connected with a Δc_p onset at, and an increase below, the onset temperature, where Δc_p is the step of heat capacity at the dynamic glass transition α. From DSC investigations in the series of poly (*n*-alkyl methacrylates) it was concluded that $\Delta c_p \sim (T_{on} - T)$, i.e. Δc_p also shows a linear onset from an extrapolated zero, $\Delta c_p = 0$ at $T = T_{on}$.

From the large slope of the continuous ($a\beta$) component above T_{on}, however, it is expected that Δc_p is not exactly zero but is very small for $T > T_{on}$. That is we expect the high-temperature *a* relaxation to have a large dielectric activity, similar to β, and a very small calorimetric activity. (We introduced the label *a* for the dispersion zone above the $\alpha\beta$ splitting[10]).

[†] Fachbereich Physik.
[‡] Fachbereich Chemie.
[⊗] Abstract published in *Advance ACS Abstracts,* October 1, 1997.

S0024-9297(96)01933-X CCC: $14.00

To be more quantitative with cooperativity, the number of particles N_α (average monomeric units for our copolymers) in a cooperatively rearranging region CRR according to Adam and Gibbs[1] is calculated by a fluctuation formula,[2,9]

$$N_\alpha = RT^2\Delta(1/c_v)/M\delta T^2 \qquad (2)$$

where $\Delta(1/c_v)$ is the step of reciprocal specific heat capacity at constant volume, M the molecular weight of the particle, and δT^2 the *ms* temperature fluctuation of a CRR. The details and the derivation of this equation and the approximations used for calculation of N_α from calorimetric data are described in ref 16.

The DSC investigations mentioned above suggested that the square root of this cooperativity has also an linear onset $N_\alpha^{1/2} \sim (T_{on} - T)$.

The random copolymers with styrene were selected for our investigations with respect to three questions.

A. Generality of the Onset and Splitting Scenario. A study of the splitting region in the relaxation chart for polystyrene PS suggests to find the onset near log ω_{on} (rad/s) $\approx 8 \pm 2$ and $T_{on} \approx 180 \pm 20$ °C. The question is how the onset for PnBMA[10] (log $\omega_{on} \approx 4 \pm 1$, $T_{on} \approx 70 \pm 10$ °C) is shifted with the styrene content of the copolymer. Another point is which of the different splitting scenarios for the poly(*n*-alkyl methacrylates)[10] is observed for the copolymers, especially if there is a change of the (possibly very specific?) PnBMA scenario having a separate onset of the α relaxation.

B. Interpretation of the Low Asymptotic WLF Frequency Constant log Ω. The analysis of the PnBMA αβ splitting scenario indicates that the asymptotic frequency of the α WLF equation, eq 1, Ω is much lower than usually observed (log Ω (rad/s) ≈7 ± 1 for PnBMA, compared to log Ω values usually in the 10−15 range). It is not possible to connect such a low Ω value with simple molecular motion on the monomeric scale (1 nm), because the thermal velocity is on the order of $v_T \approx 100$ m/s, which would give $\Omega = (100 \text{ m/s})/(1 \text{ nm}) \approx 10^{11}$/s. A second point is the $\omega_{on}/\Omega \ll 1$ relation mentioned above. If there is really such an onset, the α *cooperative* molecular motion cannot be continued beyond the onset, of course. This means that Ω cannot be interpreted as a frequency limit that is in principle accessible by the cooperative movement. We need, therefore, an entirely new interpretation of the log Ω constant or the c_1^0 constant in the WLF equation. The experimental question is how the Ω frequency shifts with the styrene content of our copolymers.

C. Dipole Compensation. The low onset frequency of PnBMA is probably connected with a specific inter and intra molecular ordering, which latter is indicated e.g. by NMR investigations.[17] The large sensitivity of the PnBMA splitting scenario to small (and hardly controllable) details[10] indicates that this ordering structure is rather delicate. The $\Delta\epsilon_\alpha$ values for PnBMA, as compared with the dipole moment density, indicate a sensitive dipole compensation mechanism connected with the cooperative rearrangements. [This compensation should not be confounded with the intensity changes of the different relaxations in the αβ splitting region.] The question is how the ordering structure, after stabilizing at small styrene contents, is disturbed and finally broken by increasing the fraction of random styrene units. We expect that $\Delta\epsilon$ increases with the styrene fraction because the subtle dipole compensation is heavily disturbed by the nonpolar styrene units.

Table 1. Sample Characteristics of PnBMA, PS, and the Random Copolymers Poly(*n*-butyl methacrylate-*stat*-styrene)

sample code	symbols used	$M_{n,total}$, kg/mol	M_w/M_n	styrene content,[a] mol %	glass temp T_g, °C
PnBMA	+ in □	520	2.12		31
2% S	■, □			2*	30
4% S	− in □			4*	31
6% S	x in □			6*	30
8% S	▲, △			8*	31
19% S	▼, ▽	250	2.10	19	33
29% S	⊡	205	2.02	29	36
38% S	◆, ◇	150	2.20	38	38
45% S	+	145	1.93	45	41
54% S	●, ○	115	2.13	54	48
60% S	⊕	115	1.91	60	53
66% S	⊖	100	2.10	66	59
76% S	⊗	96	1.98	76	67
88% S	⊙	74	2.30	88	81
PS	|	65			102
PS 700-M	×	706	1.05		101
general uncertainty		± 10%	± 0.1	± 2	±2

[a] From NMR. Data marked with an asterisk are calculated from chemical reaction parameters.

Furthermore, it is not expected that the local β relaxation of PnBMA tends continuously to the PS β relaxation, because the local mechanisms of the two homopolymers[10,18] seem to be too different.

The aim of the paper is, therefore, the complete experimental documentation of how the parameters of the WLF equation, eq 1, of cooperativity from eq 2, and of the previously obtained indications

$$\Delta\epsilon \sim (T_{on} - T),\ \Delta c_p \sim (T_{on} - T),\ N_\alpha^{1/2} \sim (T_{on} - T) \qquad (3)$$

are shifted with the styrene content of our copolymers. A few preliminary results were published in other papers devoted to special aspects of cooperativity.[16,19] A more or less closed theoretical discussion will be published elsewhere.[19]

II. Experimental Section

A. Materials. The poly(*n*-butyl methacrylate-*stat*-styrene, P(nBMA-*stat*-S)) statistical copolymers and the PnBMA homopolymer were synthesized by radical polymerization in toluene at 323 K up to a conversion of 10%. The styrene contents of the copolymers from reaction parameters and NMR[20] range from 2 to 8 mol % and from 19 to 88 mol %, respectively, and the molecular weights $\bar{M}_n$ from size exclusion chromatography SEC range from 115 kg/mol up to 250 kg/mol. SEC was based on polystyrene standards corrected for PnBMA with Kuhn−Mark−Houwink coefficients ($a = 0.758$, $K = 0.00503$ for the molecular weight range from 99 kg/mol to 1330 kg/mol). Additionally, poly(*n*-butyl methacrylate) PnBMA of comparable molecular weight was investigated. A monodisperse polystyrene PS standard (PS-700-M) with a $\bar{M}_n = 706$ kg/mol and $\bar{M}_w/\bar{M}_n = 1.05$, purchased from Waters, was also used for comparison. All samples are documented in Table 1. The dipole moment of a nBMA monomeric unit is 0.61 D (i.e. 0.20×10^{-29} As·m) and of a styrene unit 0.03 D (i.e. 0.01×10^{-29} As· m), both are calculated from the charge distribution and hybridization of a monomeric unit terminated by two methyl groups. The dipole moment of styrene is about 20 times smaller than that of *n*-butyl methacrylate.

B. Methods. 1. Dielectric Spectroscopy. A broadband dielectric spectrometer Novocontrol BDS 4000 (based on a Schlumberger 1260 frequency response analyzer) was used to measure the dielectric function, $\epsilon^*(\omega) = \epsilon'(\omega) - i\epsilon''(\omega)$, in the temperature range from 253 to 393 K and in the frequency range from $\omega = 2\pi \times 10^{-2}$ rad/s to $\omega = 2\pi \times 10^6$ rad/s. The

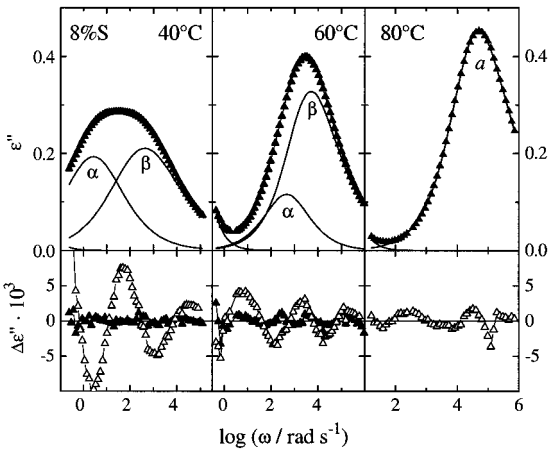

Figure 1. Example for the nonlinear least-squares fit to Havriliak−Negami HN functions. The upper part shows the dielectric loss (ϵ'') for the random copolymer with 8 mol % styrene (8% S) at temperatures 40, 60, and 80 °C as compared with the sum of a two-HN function fit T = 40 and 60 °C and a single HN function fit at 80 °C. The lower part shows the difference plots (▲, two-function fit; △, single-function fit). The jump of $\Delta\epsilon''$ at log $\omega \approx 5$ (80 °C) is due to a change of the apparatus regime.

sample capacities were about 100 pF. The samples were annealed at 403 K for 2 h before the investigations.

Using the nonlinear least-squares Levenberg-Marquard method,[21] the dielectric results were fitted by one or a sum of two Havriliak−Negami (HN) functions[22,23]

$$\epsilon^*(\omega) = \epsilon'(\omega) - i\epsilon''(\omega) = \frac{\Delta\epsilon}{\left(1 + \left(\frac{i\omega}{\omega_c}\right)^b\right)^g} + \epsilon_\infty \qquad (4)$$

subtracting a conductivity term $i\sigma_{DC}/\epsilon_0\omega^{-A}$,[24] where σ_{DC} is the temperature dependent dc conductivity and A stands for the type of conductivity ($0.1 < A \leq 1$). $A = 1$ means ionic or ohmic conductivity. ϵ_∞ is the high frequency limit of ϵ' outside the dispersion zone. The maximum loss frequency ω_{max} was analytically calculated from the fit parameters by

$$\omega_{max} = \omega_c \left[\frac{\sin\frac{\pi}{2}b}{\tan\frac{\pi b}{2(g+1)}} - \cos\frac{\pi}{2}b \right]^{-1/b} \qquad (5)$$

For $\omega \ll \omega_{max}$ and $\omega \gg \omega_{max}$ the HN function for ϵ'' reduces to power laws with exponents b and $-bg$,[25] respectively.

An alternative approach for the analysis of the splitting behavior would be the Williams formula $\phi(t) = a\phi_\alpha(t) + (1 - a)\phi_\beta(t)\phi_\alpha(t)$[26] used e.g. in ref 27 for liquid Bisphenol-C−dimethyl ether (BCDE) and polybutadiene.[28] This approach, however, favors a special splitting scenario with a continuous $\alpha\beta-\alpha$ (or $a-\alpha$ in our terms) trace in the Arrhenius diagram which is surely not realized in PnBMA.[10]

Representative examples of the fit of ϵ'' by one or a sum of two HN functions and a conductivity term were checked by a difference plot (Figure 1). The single HN function fit was replaced by a two HN-functions fit and restarted with new start parameters, if the one-HN deviation plot shows a significant peak structure.

The difference plot for the 80 °C isotherm shows a step at 10^5 rad/s resulting from a switch in the dielectric analyzer at this frequency. At T = 80 °C this disturbance is near the maximum of ϵ''. For lower temperatures this disturbance is on the high-frequency flank of the β process and does not disturb the peak analysis.

As a rule, all eight HN function parameters ($\Delta\epsilon$, ω_c, b, g for α and β) were freely adjusted. The two exceptions are as follows. (i) For samples up to 38 mol % styrene the α process fit parameter g was fixed to 1 (symmetrical dispersion zone). (ii) For samples with equal or more than 19 mol % styrene, the β process shape parameter bg in the splitting region was fixed to values calculated from a linear extrapolation of low-temperature values outside the splitting region. This procedure was checked for samples with small styrene content where bg decreases linearly with increasing reciprocal temperature. These moderate restrictions stabilize the fit procedure and do not favor a special scenario.

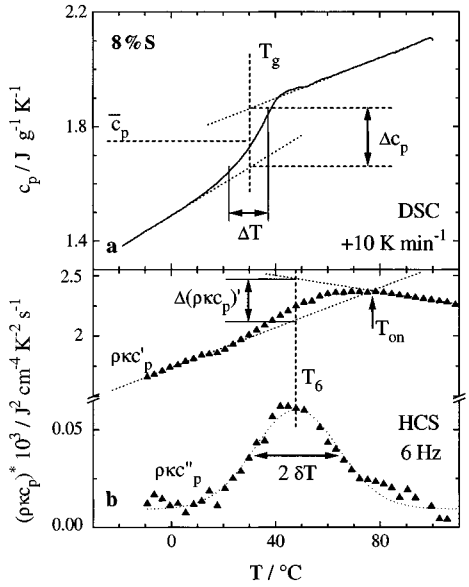

Figure 2. Estimation of glass transition parameters (T_g, δT, $\bar{c}_p$, Δc_p) and onset temperature T_{on} from DSC (a) and HCS (b) for the 8% S copolymer sample. T_6 is the heat capacity loss maximum temperature at frequency f = 6 Hz.

2. Differential Scanning Calorimetry (DSC). A DSC 7 apparatus (Perkin Elmer), was used with cooling and heating rates of $|dT/dt|$ = 10 K min^{-1}. The sample masses were between 8 and 11 mg, and the annealing time between heating and cooling was 10 min.

The glass transition temperature T_g was calculated by an equal-area construction using the two tangents below and above T_g (Figure 2a). The scatter of T_g from different runs is about 2 K. The Δc_p step height was obtained from the tangent distance at T_g. The temperature width ΔT of the c_p step is taken between 16% and 84% of the total step height.

3. Heat Capacity Spectroscopy (HCS). The frequency dependence of the product of mass density, thermal conductivity, and heat capacity, $(\rho\kappa c_p(\omega))^*$, is measured by a heat capacity spectrometer. The product was decoupled assuming that the thermal conductivity κ and density ρ has no dispersion, i.e. $(\rho\kappa c_p(\omega))^* = \rho\kappa c_p'(\omega) - i\rho\kappa c_p''(\omega)$.

The central part of the heat capacity spectrometer is a thin (70−100 nm) nickel heater on the surface of a thick (4 mm) substrate of poly(ether ether ketone), PEEK. The dimensions of the nickel stripe are about 1 × 5 mm^2. The heater has a high temperature coefficient of electrical resistance (≈(1−2) × 10^{-3} K^{-1}) and is also used as the thermometer. This assembly was coated with the sample after a reference measurement for the determination of the heater and substrate parameters. The sample thickness was about 1.5 mm. Further details of the spectrometer are published in ref 29.

The quantity $(\rho\kappa c_p(\omega))^*$ was isothermally measured at nine frequencies $\nu = \omega/2\pi$ between 0.2 and 2000 Hz beginning at the highest temperature. The annealing time at each isotherm prior to measurement was 900 s. Figure 2b shows the real and imaginary part of $(\rho\kappa c_p(T))^*$ for the 8% S sample at a frequency of 6 Hz.

The imaginary part, $\rho\kappa c_p''(\omega, T)$ as a function of temperature, was fitted by a Gauss function to determine the α relaxation temperature as the curve maximum, T_ν, and the dispersion, δT (Figure 2b).

The step height, $\Delta c_p(T)$, and the mean heat capacity at $T_\nu = T_g(\nu)$, $\bar{c}_p$, were estimated from the real part of $\rho\kappa c_p'(T)$ in a manner similar to that for DSC results. The absolute values of $\Delta c_p(T)$ and $\bar{c}_p$ are calculated from HCS after gauging with DSC at temperatures above the dispersion zone.

Table 2. Comparison of Onset Temperatures T_{on} Estimated by Various Methods[a]

sample code	intersection method	$\Delta\epsilon_\alpha \rightarrow 0$	$\Delta c_p \rightarrow 0$	$N_\alpha^{1/2} \rightarrow 0$	average
2% S	86 °C	68 °C	85 °C	81 °C	78 °C
8% S	87 °C	74 °C	88 °C	87 °C	83 °C
19% S	97 °C	103 °C	104 °C	93 °C	100 °C

[a] Key: (1) intersection method (Figure 2b); (2) linear extrapolation of $\Delta\epsilon_\alpha$ to zero ($\Delta\epsilon_\alpha \rightarrow 0$); (3) linear extrapolation of Δc_p to zero ($\Delta c_p \rightarrow 0$); (4) linear extrapolation of $N_\alpha^{1/2}$ to zero ($N_\alpha^{1/2} \rightarrow 0$, Figure 5). The average is without the intersection method. The general uncertainty is about ±10 K.

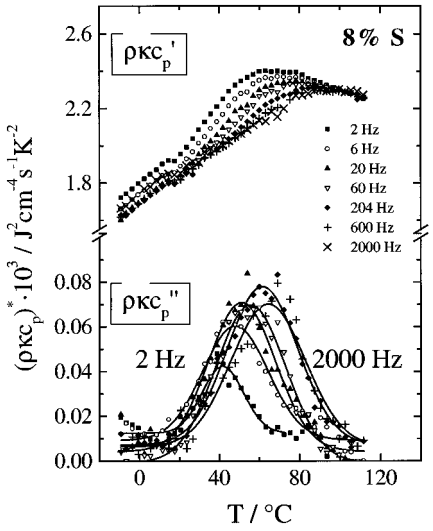

Figure 3. Heat capacity spectroscopy HCS $(\rho\kappa c_p)'$ (a) and $(\rho\kappa c_p)''$ (b) curves as a function of temperature with parameter frequency for the 8% S copolymer sample.

The intersection of the two tangents outside the dispersion zone gives an estimate of the onset temperature, T_{on} (Figure 2b). These intersection-method values for our copolymers are compared with T_{on} values from extrapolations using eq 3 (Table 2).

III. Results

The real-part HCS isochrons for the 8% S copolymer have a step ($\Delta c_p > 0$) for lower frequencies (temperatures) that degenerates to a bend ($\Delta c_p \rightarrow 0$) for higher frequencies (Figure 3a). The slope dc_p'/dT in the glass zone (below the dispersion) is significantly larger than the slope in the liquid zone (above the dispersion). This permits the intersection method for the determination of the onset temperature, mentioned above, and indicates that the kinetic structure of the glass zone changes considerably when the onset is approached. The peak of the imaginary part isochrons shifts to higher temperatures for increasing frequency. The peak position (ω_{max}, T_{max}) and the temperature dispersion δT can be determined from the Gauss fits of Figure 3b with a general uncertainty of $\Delta T_{max} = \pm 3$ K and $\Delta(\delta T) = \pm 3$ K. The δT uncertainty is much larger for isochrons where the basis line at large and low temperatures is ill-defined because of contact problems between the sample and the nickel heater.

The dielectric Arrhenius diagram for the same sample (with the ϵ'' peak maximum frequencies) shows the $\alpha\beta$ splitting scenario of PnBMA[10] (Figure 4a). A high-temperature process *a* is continuously connected with the local Johari−Goldstein β process, with respect to both the trace and the relaxation intensity, $\Delta\epsilon$ (Figure 4b). The α relaxation intensity, $\Delta\epsilon_\alpha$, has an onset with $\Delta\epsilon_\alpha = 0$ and increases linearly with falling temperature. The α trace in the Arrhenius diagram does not touch

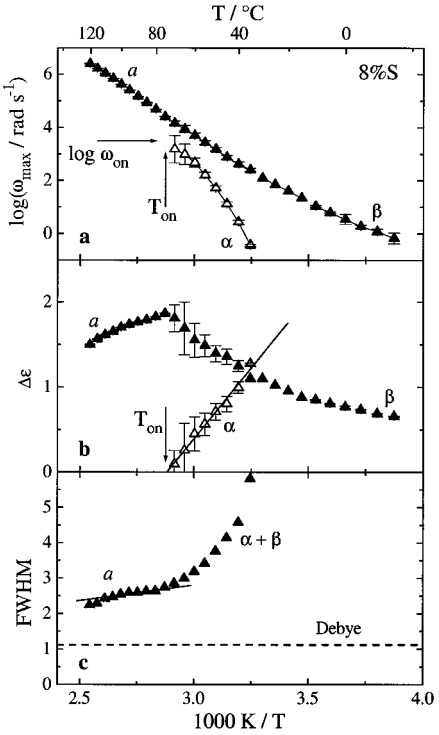

Figure 4. Arrhenius diagram (a), dielectric intensities $\Delta\epsilon$ of α, β, and *a* process (b), and fwhm of the whole dispersion zone (c) of the 8% S copolymer. The onset temperature T_{on} is estimated by linear regression in part b. The fwhm is the half-width $\Delta(\log_{10}\omega)$ of the ϵ'' peak.

the continuous $a\beta$ trace. Instead the α onset is about one frequency decade below the continuous $a\beta$ trace. This gap is outside the experimental uncertainty.[30] In contrast to the PnBMA scenario of ref 10, where the continuous $a\beta$ trace is exactly a straight line in the Arrhenius diagram ($-3 < \log\omega < +6$), this trace has a slight bend for the 8% S copolymer (and, by the way, for other homo PnBMA samples, too).

The onset temperature is also marked in the total half-width (fwhm, Figure 4c) of the total ϵ'' peak as a function of temperature, without making an analysis for the components. Below the onset this half-width increases abruptly. An inspection of the original ϵ'' data shows that it is the low-frequency flank (the α side) that is responsible for this increase.

The HCS results (only α active) and the dielectric results (active for *a*, α, and β) are compared for three (2% S, 8% S, and 19% S) copolymers in Figure 5. The dielectric splitting scenario is the same for all three samples (upper part of Figure 5). Some decades below the onset frequency, the HCS trace (ω_{max} of the c_p'' peak as a function of temperature) is near the dielectric trace. Such a behavior was also observed in amorphous homopolymers as polystyrene PS, polyvinylacetate PVAC, and natural rubber NR.[31,32] Near the onset, however, the HCS trace (open symbols) changes from the α to the $a\beta$ trace. Unfortunately this trend cannot be followed to higher frequencies since our HCS apparatus is only operating up to about 2 kHz. The present HCS sensitivity does not allow to detect any $a\alpha$ splitting of the c_p'' trace. The dielectric intensities ($\Delta\epsilon_a$, $\Delta\epsilon_\alpha$, $\Delta\epsilon_\beta$) also behave similarly for all three samples (middle part of Figure 5). The calorimetric intensities $\Delta c_p'$ for α are also linear functions of temperature and indicate a steep onset behavior. Unfortunately the distance of the nearest Δc_p value to the extrapolated zero onset is relatively large, so that the onset temperature must be

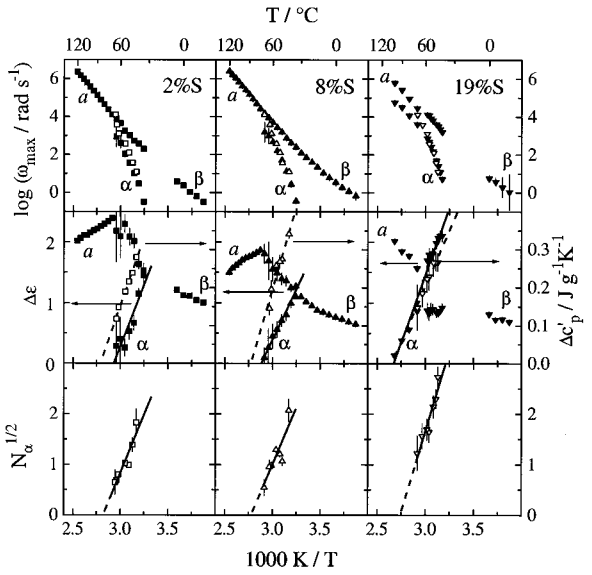

Figure 5. Comparison between dielectric (solid symbols) and HCS (open symbols) results for the random copolymers with 2, 8, and 19% styrene. The upper diagrams show the Arrhenius diagrams, the middle diagrams compare the dielectric intensities $\Delta\epsilon$ with the HCS step heights Δc_p, and the lower diagrams show the square root of particle number per cooperatively rearranging region CRR, $N_\alpha^{1/2}$.

calculated by linear regression and extrapolation over large temperature differences (about 20 K).

The square root of cooperativity (lower part of Figure 5) was calculated from eq 2 using the approximation[16]

$$\Delta(1/c_v) \approx \Delta c_p/\bar{c}_p{}^2 \tag{6}$$

It is the square root, $N_\alpha^{1/2}$, that shows a linear onset behavior, $N_\alpha^{1/2} \sim (T_{on} - T) \rightarrow 0$, with onset temperatures that are comparable with those calculated from linear regressions of $\Delta\epsilon \rightarrow 0$ and $\Delta c_p \rightarrow 0$, as well as from the intersection method (Table 2). The $N_\alpha^{1/2}$ onset is not only determined by the Δc_p behavior but also by considerable changes of the δT dispersion near the onset. The square root is interpreted by the dominance of fluctuation for small CRR's containing only a few particles.[33]

Both trends, $\Delta c_p \rightarrow 0$ and $N_\alpha^{1/2} \rightarrow 0$, are clear indications that we really have a *cooperativity* onset in the $\alpha\beta$ splitting region. The minimal cooperativity observed is on the order of $N_\alpha = 1$ which does not mean that cooperativity can be operating with one monomeric unit.[33] The frequency limit ($\nu \lesssim 2$ kHz) and the sensitivity limit ($\Delta c_p/\bar{c}_p > 1\%$) of our HCS apparatus do not exclude that the high-temperature *a* process has a small, nonzero cooperativity, as indicated by the $a\beta$ trace change of the HCS symbols in Figure 5, mentioned above.

DSC curves at a given cooling/heating rate (e.g. 10 K/min, without annealing between) correspond to a frequency of about 1 mHz.[34] Increasing the styrene content means enlarging the log frequency distance to the onset, $\log(\omega_{on}/2\pi \times 10^{-3}/\text{s})$. The DSC curves of cooling−heating cycles without annealing, i.e. the glass temperatures, are shifted to higher temperatures and show a significant narrowing of the transformation interval ΔT (Figure 6a for the heating phase after cooling with equal rate). If the chemical heterogeneity would be the main effect, contrarily a widening for increasing styrene content up to about 50% S is to be expected. Combining the DSC parameters by eq 2, however, we find that the cooperativity is systematically

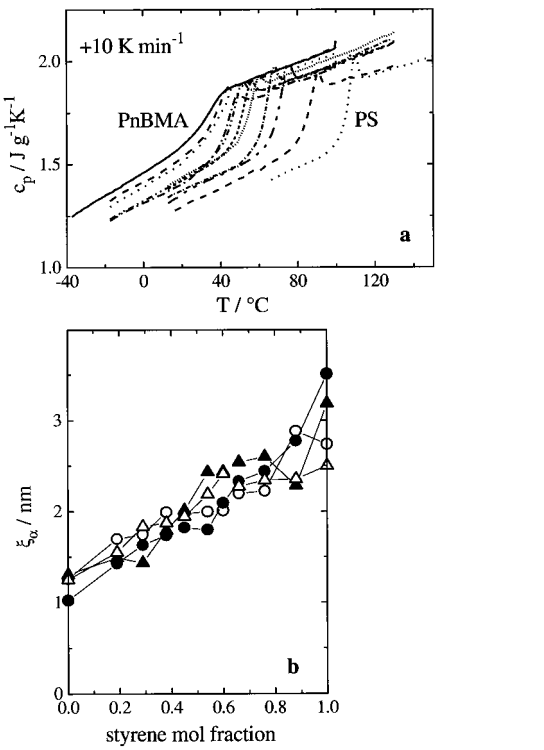

Figure 6. (a) DSC heating traces for the copolymers of Table 1 except 2% S, 4% S, 6% S, and 8% S. (b) Characteristic lengths ξ_α (eq 7) for PnBMA, PS, and the series of copolymers calculated from DSC for two independent heating (solid symbols) and cooling (open symbols) runs. The scatter indicates the general uncertainty.

increased from PnBMA to PS (Figure 6b). The characteristic length was calculated from $\xi_\alpha = V_\alpha^{1/3}$, where V_α is the CRR volume, calculated from N_α by

$$\xi_\alpha{}^3 = \mathrm{V}_\alpha = N_\alpha M_0/\rho \tag{7}$$

Besides the eq 2 approximation we used a crude correction of structural relaxation for estimation of δT from the DSC 16%−84% ΔT transformation intervals:[16,36]

$$\begin{aligned} \delta T &= \Delta T/2.5 \qquad \text{for heating} \\ \delta T &= \Delta T/4 \qquad \text{for cooling} \end{aligned} \tag{8}$$

The increase of ξ_α with the styrene fraction is interpreted as some map of the general temperature dependence $\xi_\alpha(T)$ for one sample to the composition dependence for different samples via the change of the onset distance.

The qualitative type of the dielectric splitting scenario does not change from 0% S up to 54% S (Figure 7). All these samples show a separate α onset about one frequency decade below the continuous $a\beta$ trace for the local process. This means that this scenario is not restricted to the possibly very special molecular ordering in PnBMA. Above 54% S the splitting region is above the frequency window of our apparatus. Some splitting details at medium styrene fractions will be described in the Appendix.

The α traces in the Arrhenius diagram are curved and we can determine a WLF equation for each styrene content (Table 3). Determining T_{on} by the $\Delta\epsilon_\alpha \rightarrow 0$ method mentioned above, we can determine the onset frequency ω_{on} from eq 1

$$\log \omega_{on} = \log \Omega - B/(T_{on} - T_\infty) \tag{9}$$

Table 3. Dielectric α process properties: Vogel Temperature T_∞, WLF Limit Frequency log Ω = $\log_{10}$ Ω, VFT Parameter *B* (Equation 1), Onset Temperature T_{on} (Table 2, Second Column), Onset Frequency log ω_{on} (Equation 7), Half-Width δ_0 log ω of the Dielectric Loss peak at the Onset, $\Delta\epsilon_\alpha$ Intensity Slope vs 1/*T*, and the Fragility Parameter $F = T_g/(T_g - T_\infty)$

sample code	T_∞/°C	log Ω, rad/s	*B*, K	T_{on}, °C	log ω_{on}, rad/s	δ_0 log ω	d($\Delta\epsilon_\alpha$)/ d(1000 K/*T*)	*F*
PnBMA	4	7	232	75	3.7	1.39	1.9	*b*
2%	−7	7.2	318	68	3	1.5	5.55	7.2
4%	−7	7.5	320	75	3.9	1.21	4.1	7.8
6%	−13	8	396	83	3.9	1.36	2.54	6.8
8%	−9	8	375	74	3.5	1.56	3.31	7.3
19%	−4	8	323	103	4.7	1.41	4.12	8.3
29%	−15	9.5	520	113	5.4	1.38	3.8	6.1
38%[c]	11	7.5	284	98	4.4	1.44	6.4	11.5
38%[c]	2	8.8	398	127	5.5	1.32	1.8	8.6
54%	−4	10	533	133	6.5	1.28	5.77	6.2
60%	8	10.7	531	150	6.5	1.47	3.4	7.2
88%	27	13.4	781	*d*	*d*	*d*	*b*	6.6
PS 700-M	78	9.1	351	*d*	*d*	*d*	*b*	*b*
general uncertainty[a]	±10K	±1	±150	±10K	±1	±0.2	±0.5	±1

[a] Larger uncertainties of several values are indicated in the diagrams by larger error bars. [b] Could not be determined in our apparates by various causes. [c] The upper line is for α_2, and the lower line, for α_1; see Appendix. [d] Too far outside the frequency window.

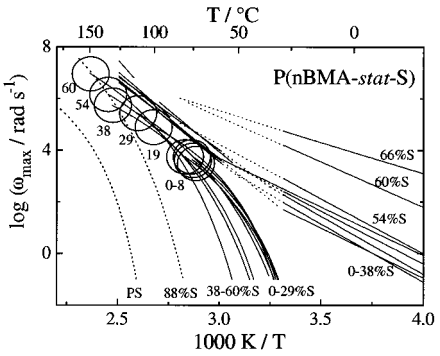

Figure 7. Overview of the Arrhenius diagrams of all samples dielectrically investigated. The center of the circles mark the onset temperature T_{on} and onset frequency log ω_{on}; their radii approximately represent the onset uncertainty. The gaps for the local processes (partly dotted) are explained in the caption of Figure 4. The circle for the 38% S sample is for α_1 (Appendix, Figure 12a); the α_2 circle of the 38% S sample would be near the circle for the 19% S sample.

The onset temperature T_{on} is an almost linear function of the styrene content, whereas the glass temperature T_g and the Vogel temperature T_∞ are typically curved functions of the styrene content that can well be fitted by Gordon−Taylor equations (Figure 8a). The extrapolated onset temperature for polystyrene would be $T_{on} \approx 195 \pm 10$ °C. This should be compared with an $\alpha\beta$ intersection at $T = 150$ °C obtained from NMR methods.[35] Both T_g and T_∞ are nearly constant up to about 30% S. If T_g is interpreted by the ratio of energy/entropy changes, $T_g = \Delta H/\Delta S$, this finding can be explained by a compensation of the energy gain from styrene units vs a loss of PnBMA order from the random copolymerization.

Most interesting is the low asymptotic WLF frequency Ω for low styrene content (Figure 8b), log Ω (rad/s) = $\log_{10}$ Ω ≈ 7. Both log Ω and the onset mobility, log ω_{on}, are almost linear functions of the styrene fraction with the property that their ratio is nearly constant

$$\log(\Omega/\omega_{on}) = 3.8 \pm 1 \qquad (10)$$

independent of the styrene fraction (≤60 = % S). The extrapolated values for PS are log ω_{on}(rad/s) 8.6 ± 1 and log Ω = 12.6 ± 2.

The steepness of the dielectric α onset, i.e. the slope $-d\Delta\epsilon_\alpha/dT$ or $d(\Delta\epsilon_\alpha)/d(1/T)$ increases by an average factor of 2 between 0 and 20% styrene (Figure 8c). It is remarkable that the steepness increases by random copolymerization with a nonpolar component. This is interpreted as a disturbance of the dipole compensation in the α relaxation of PnBMA. The increase seems to show some irregularity outside the experimental uncertainties for small styrene mole fractions, e.g. for 2% S. This corresponds to the observation that the splitting scenario of homo PnBMA is very sensitive to details of the synthesis and aging. Both findings indicate a delicate molecular order causing the dipole compensation. Figure 8c also indicates that the slope decreases for higher styrene fraction, as expected since the dipole moment of styrene is small.

The ϵ'' peak half-width of the α relaxation can be extrapolated to the onset. The values obtained are slightly above a Lorentz line, $\delta_0 \log \omega = 1.14$ (Table 3). This means that the dielectric activity of the cooperative α dispersion starts approximately with a Debye relaxation.

As mentioned above, the high-temperature part of the continuous trace in the Arrhenius diagram is labeled by *a*, the low temperature part (here: below the bend indicated in Figures 4 and 5) by β (Johari−Goldstein process). The parameters of the β relaxation are collected in Table 4, including the formal linear extrapolation of log ω_β for $1/T \rightarrow 0$. The values obtained for the log ω_β(rad/s) limits are between 13 and 17. This is compatible with a local nature of the β process, for which a value of about 14 is expected.[37] Above the $a\beta$ bend, the activation energy E_A^a is larger (Table 4), and the log ω_a extrapolations for $1/T \rightarrow 0$ give larger values, both indicating some cooperativity for the high-temperature *a* process.

The linear β trace in the Arrhenius diagram is systematically shifted to higher frequencies for increasing styrene fractions up to 66% S—away from the β trace of polystyrene (Figure 9a). It is not very probable that this trend is inversed for higher styrene fractions. Instead we expect that there is no continuity of the β processes for PnBMA and PS. Such a discontinuity is often observed in other copolymer systems, e.g., for P(MA-*stat*-MMA).[37] Up to 29% S the β half width (fwhm) is about 5−6, but for higher styrene fractions up to 66% S the β dispersion zone is very broad (Figure 9b), especially at low temperatures. For higher styrene fractions the randomness of chemical configuration causes a lot of different environments for the local process, with a corresponding broad distribution of activation energies.

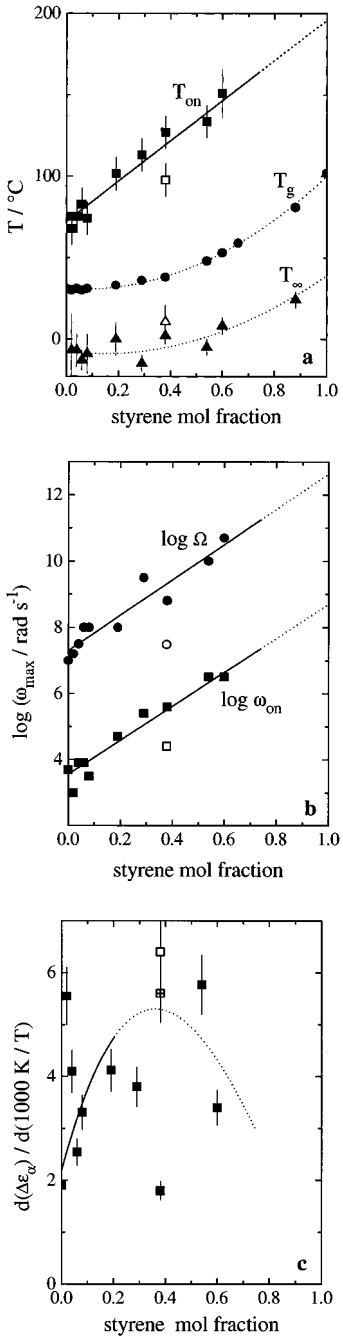

Figure 8. (a) α process temperatures (DSC glass temperature T_g, Vogel temperature T_∞, onset temperature T_{on}) as a function of the styrene content. The open points for the 38% S sample are for α_2 (Appendix, Figure 12a). (b) Onset frequency log ω_{on} (eq 9) and WLF asymptotic frequency log Ω (eq 1) as a function of the styrene content. (c) α process intensity slope $d(\Delta\epsilon^\alpha)/d(1/T)$ as a function of the styrene content. The irregularities are probably outside the uncertainties. The open point for the 38% S sample is for α_2 and the + in □ symbol results from linear extrapolation considering all points (Appendix, Figure 12b).

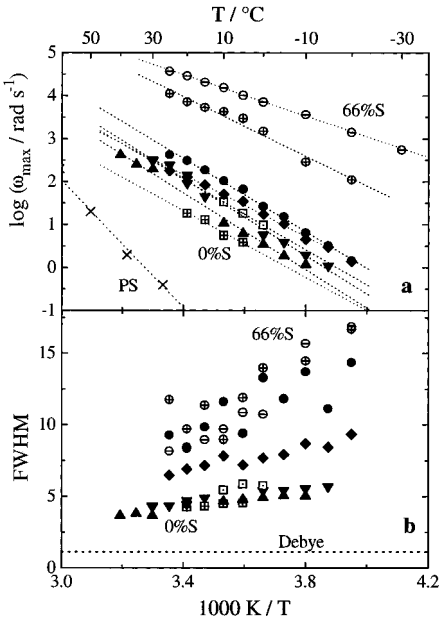

Figure 9. (a) Arrhenius diagram of the β relaxation for PnBMA, PS (data from ref 16), and several random copolymers. The dotted lines represent linear regressions below the bend (Figures 4, 5, and 7) of the continuous $a\beta$ traces. (b) β-process fwhm vs reciprocal temperature for the same samples. The dotted line shows the Lorentz line arising from the relaxation of a Debye relaxator (fwhm = 1.14).

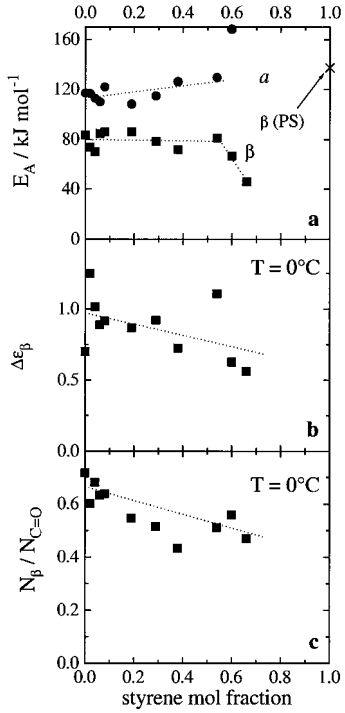

Figure 10. (a) *a* process and β process activation energies (E_A^a, E_A^β) as a function of the styrene content. (b) β-process intensity $\Delta\epsilon_\beta$. (c) Number of active dipoles per number of carboxyl groups.

The average β activation energy remains nearly constant, $E_A^\beta \approx 80$ kJ/mol up to 55% S. This means that the average energy barrier is made by the nBMA monomers. Then the activation energy decreases, obviously by the disturbance due to the random, frequent styrene units (Figure 10a). The trend is again away from the β polystyrene activation energy, which is much higher, about 135 kJ/mol. This is a further indication for two different local mechanisms. The high-temperature process activation energy E_A^a is significantly higher than for β ($E_A^a \approx 120$ kJ/mol), but similar to the apparent activiation energy for the α process at the onset temperature T_{on}, E_A^α (cf. Table 4). The β dielectric relaxation strength does not have any dramatic change (Figure 10b).

The number density of β activated dipoles is estimated from the Debye formula[38]

$$N_\beta = \frac{9\epsilon_0 k_B T}{\mu^2}\left(\frac{\epsilon(0)-1}{\epsilon(0)+2} - \frac{\epsilon_\infty - 1}{\epsilon_\infty + 2}\right) \qquad (11)$$

with $\epsilon(0) = \Delta\epsilon_\beta + \epsilon_\infty$ and $\mu = 0.97$ D (assuming that the

Table 4. Dielectric β and a Process Properties: Activation Energies E_A^β, E_A^a, and $E_A^\alpha(T_{on})$, Extrapolated Limit Frequency log ω_β (rad/s) for $T \to \infty$; Logarithmic Half-Width fwhm, Dielectric Intensity $\Delta\epsilon_\beta$, the Number of β Relaxing Side Groups per nm^3, and Its Percentage As Compared to the Total Number of nBMA Side Groups, N_β/N_{nBMA} at 0 °C

sample code	E_A^a, kJ/mol	$E_A^\alpha(T_{on})$, kJ/mol	E_A^β, kJ/mol	$\lim_{T\to\infty}$ log ω_β	fwhm (0 °C)	$\Delta\epsilon_\beta$ (0 °C)	ϵ_∞ (0 °C)	N_β (0 °C)	N_β/N_{nBMA} (0 °C)
PnBMA	117	129	83.5	14.5	4.6	0.7	2	3.2	0.72
2%	117	142	74	14.5	4.8	1.25	3.8	2.6	0.6
4%	113	167	70	14	4.7	1.02	3	2.9	0.68
6%	110	104	86	17.1	4.9	0.89	2.9	2.7	0.63
8%	122	127	86	16.9	4.9	0.92	3	2.7	0.64
19%	108	103	86	17.2	5.4	0.87	3.6	2.1	0.54
29%	115	114	78.4	16	5.8	0.92	4.3	1.75	0.52
38%	126	121	71.9	15	7.7	0.73	4.6	1.3	0.43
54%	130	115	81.2	17	(13.3)	1.11	6.3	1.23	0.51
60%	168	*b*	66.9	15.8	(14.0)	0.63	4.5	1.17	0.56
66%	*b*	*b*	45.9	12.7	(10.7)	0.56	5.3	0.84	0.47
PS 700-M	*b*	*b*	137.6[c]	24.1[c]	*b*	*b*	2.5	*b*	*b*
general uncertainty[a]	±10	±10	±5	±1	±0.2	±10%	±10%	±20%	±20%

[a] Larger uncertainties of several values are indicated in the diagrams by larger error bars. [b] Could not be determined in our apparates by various causes. [c] From mechanical data quoted in ref 18, p 414.

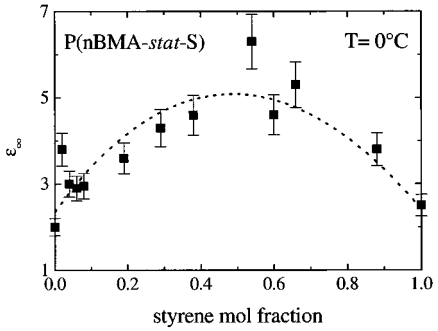

Figure 11. High-frequency (>MHz) values beyond β of the real part of the dielectric function ϵ_∞ as a function of the styrene mole fraction for $T = 0$ °C. The dotted line is only a guide for the eye.

dipole moment of the carboxyl group is relevant for β). The number density of $C=0$ bonds, $N_{c=0}$, is calculated from the density and the nBMA fraction. The ratio $N_\beta/N_{c=0}$ is about 0.6, nearly constant for all styrene fractions investigated (Figure 10c). This means that our average β process is generated by the nBMA units in the same manner, independently from the styrene fraction. [For $\mu = 0.61$ D (as estimated above for the nBMA unit) the ratio N_β/N_{nBMA} would be about 1.5 > 1. This is, of course, not possible.]

The high-frequency (>10 MHz) limit ϵ_∞ of the dielectric function has a pronounced maximum at about 50% S (Figure 11). Since the electronic polarization is additive, this means that the dipoles must take part at molecular motions for >10 MHz frequencies. The maximum indicates that disturbing of dipole compensation by the nonpolar styrene units plays also a role for these fast relaxations. We suggest that some kind of γ relaxation[39] is responsible for this ϵ_∞ (>10 MHz) behavior.

IV. Discussion and Conclusion

The discussion is along the three questions of the Introduction.

A. Generality of the Onset and Splitting Scenario. After the PnBMA type $\alpha\beta$ splitting scenario was published [with a continuous $a\beta$ trace in the Arrhenius diagram[10] and continuous a and β intensity, connecting the high-temperature relaxation (a) and the low-temperature local β relaxation, and a discontinuous onset of the cooperative α relaxation, separated by a gap of about one frequency decade below $a\beta$], many people objected that this should be a peculiarity connected with a highly special molecular ordering in PnBMA. Since such an ordering must heavily be disarranged by the randomly distributed styrene units along the chains, our finding that both the type of scenario and the linear onset character does not change up to a styrene fraction of 54% S (Figures 5 and 7) proves that this scenario is not restricted to a special molecular order. It is only the parameters of the scenario that change in an unexpectedly wide range.

This does not mean, however, that our scenario is the only one that can occur, because at least one other scenario was even observed in the poly(*n*-alkyl methacrylates) series, e.g. for PEMA and probably for the propyl member.[10] It is an open question whether a scenario change occurs beyond 54% S and if our scenario is also observed for the homopolymer polystyrene.

As mentioned above, it was suggested that for BCDE another scenario can be seen by high-frequency dielectric spectroscopy.[27] Unfortunately, a formula was there used for analyzing the splitting scenario that is biased with respect to different scenarios. Moreover some experimental indications of steeply falling α intensity in the splitting region were not discussed with respect to other scenarios.

An open question is if the dielectric and the calorimetric onset is exactly the same. The large uncertainty of the extrapolated T_{on} values (±10 K, Table 2 and Figure 5) does not exclude that both activities mark a common onset. On the other hand, careful shear and dielectric investigations of the highly sensitive homo PnBMA indicate that different activities can have a different onset behavior.[15,14] This point needs further investigations in substances, where the beyond-onset range is commonly accessible by different activities, e.g., oligomers of PnBMA and PEMA as suggested by Beiner[40] and Reissig.[41]

B. New Interpretation of the log Ω WLF Asymptote. The conventional interpretation of the log Ω (or $c_1^0 = \log(\Omega/\omega_0)$) WLF constant is that this is a high frequency of molecular motion that is in principle accessible by a typical α motion for high temperatures. Our experimental findings imply, at least for our copolymer series, that such an interpretation is not universally possible, for two reasons: First, the cooperative α motion ends with a nearly zero intensity at an onset frequency far below the WLF asymptote, $\log(\Omega/\omega_{on}) \approx 4$ (Figure 8b). This effect is not singular for PnBMA but is systematic for our copolymer series. This means that log Ω cannot be reached by the α motion,

even not in principle. Second, the Ω frequency for small styrene fractions is in the megahertz range that cannot be explained by the simple estimation "thermal velocity $v_T \approx 100$ m/s divided by intermolecular distance of order one nanometer".

This small Ω situation cannot be compared with the small WLF asymptote for the flow transition[42] that can systematically be lowered to very small values by enlarging the chain length M, $\log \Omega \sim -3.4 \log M$. There we have a new molecular mechanism, e.g. fluctuative disentanglement by tube renewing, that is connected with a new kinetic structure (entanglement) stable up to very high frequencies in the gigahertz range.[43] [If there is an onset of some kind of cooperativity with the flow transition, then it must be understood on the basis of this fluctuating but permanent kinetic structure.]

A new interpretation of log Ω for the dynamic α glass transition is suggested on the basis of the concept of "kinetic molecular randomness".[16,19,33] The idea is that the high thermal velocity $v_T \approx 100$ m/s generates many local chances for elements of the cooperative rearranging. Their frequency is denoted by Ω′. Cooperativity becomes necessary for decreasing free volume. We assume that the related fluctuation is necessary for the molecular α transition and that *only a small part of these chances can randomly be used for real cooperative rearrangements*. Their frequency is denoted by $\omega_\alpha \equiv \omega$, with $\omega \ll \Omega'$. The new interpretation puts $\Omega = \Omega'$; i.e., the asymptotic WLF frequency is interpreted as the frequency for the *chances*.

Comparing with the local β process, we see significant differences. For β, the limit frequency ω_β (for high temperatures) is interpreted by the number of attempts per second to overcome the activation barrier. This limit can be estimated by the simple method mentioned above. The actual β frequency ω_β at lower temperatures is then the frequency of the overcoming success, and for local processes there is no in principle argument against continuity to the limit when $1/T \rightarrow 0$. For cooperativity based on kinetic molecular randomness, however, the situation is characterized by a new property that can only be established for $\omega \ll \Omega$, implying also $\omega_{on} \ll \Omega$. The onset behavior observed in our copolymer shows that the new property, i.e., the cooperativity, emerges discontinuously, if a possible crossover is neglected. That is we do not have a continuity to the Ω limit frequency.

As yet there are only a few systematic investigations of log Ω or c_1^0. In polymers such PVAC, PS, and NR, log Ω depends on the activity: It is higher for shear modulus G^* than for ϵ^* and c_p^*.[31] This is interpreted by some scaling inside the main dispersion zone, i.e. that there are less chances for larger-scaled motions inside a cooperativity region.

The low Ω values observed in our samples should be explained by a molecular situation where some molecular ordering results in a considerable decrease of local chances for cooperativity elements. Glass transition cooperativity is, of course, connected with molecular disorder, since high order, generally spoken, prevents glass transition.

With regard to a discussion of the small values of minimal cooperativity near the onset, $N_\alpha^{min} \approx 1$, the reader is referred to the theoretical paper.[19]

C. Dipole Decompensation. Having no molecular order in mind that prefers a certain degree of mutual compensation of neighboring electric dipoles (⇅ in the simplest case), we would expect that random mixing with a weakly or nonpolar component decreases the intensity of dielectric properties. In our systems, however, starting from a weakly syndiotactic PnBMA (T_g = 31 °C) we observe the opposite (Table 4, Figures 8c and 11). Dielectric spectroscopy allows some dielectric classification of the different modes below the $\alpha\beta$ splitting temperature: cooperative α, local β, and high-frequency >10 MHz hypothetical γ motion, characterized by $\Delta\epsilon_\alpha$, $\Delta\epsilon_\beta$, and the dipole part of ϵ_∞, respectively. The considerable increase of the dielectric activity for α and ϵ_∞ with the styrene fraction (up to about 50% S) proves that both the cooperative α and the hypothetical γ relaxation (perhaps some kind of PE-like glass transition[39] with participation of a certain fraction of the dipoles) are characterized by a kinetics that prefers dipole compensation. Increasing chemical disorder disturbes this compensation. This explains increasing dielectric activity although the random styrene units do not have a dipole moment worth mentioning. The local β process has no such a decomposition effect, as expected (cf. the $\Delta\epsilon_\beta$ values of Table 4).

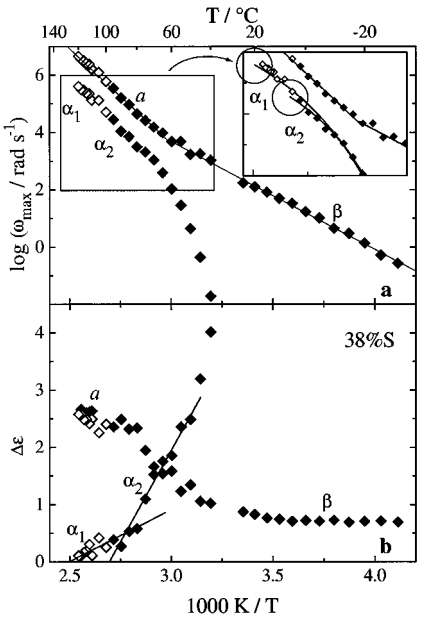

Figure 12. Arrhenius diagram (a) and dielectric intensities $\Delta\epsilon$ (b) of the *a*, α, and β processes for the 38% S copolymer (analogously to Figures 4 and 5). The open symbols correspond to a very weak α process and have larger uncertainties than the full symbols. The division of α into α_1 and α_2 is tentative; see text. The inset shows the WLF fits with (α_1) and without (α_2) the open symbols.

Acknowledgment. The financial support of the Land Sachsen-Anhalt, the Deutsche Forschungsgemeinschaft DFG, and the Fonds der Chemischen Industrie is gratefully acknowledged. Furthermore, we thank Dr. H. Menge for the NMR measurements to estimate the styrene content, and Dr. J. Giesemann (Fachbereich Chemie, Universität Halle) for his suggestion to investigate the styrene copolymers.

Appendix

This appendix is to discuss some details of the α onset for a sample with medium styrene fraction. The continuous $a\beta$ trace in the Arrhenius diagram for the 38% S copolymer (Figure 12a) has a clear bend at about T = 65 ± 5 °C that can be used for a distinction between high-temperature *a* and local β process. The *a* process has a limit frequency $\lim \log \omega_{max}^a \approx 22$ (rad/s) for $1/T \rightarrow 0$, indicating some nonlocality of *a*. Including less

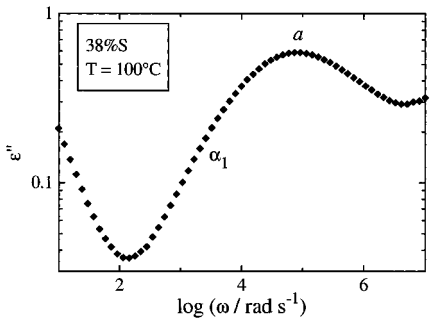

Figure 13. Original experimental ϵ'' points for the 38% S copolymer at $T = 100$ °C, above the extrapolated onset temperature for the α_2 relaxation, $T_{on}(\alpha_2) \approx 95$ °C. The left flank shows a bend at α_1 that cannot be fitted by one HN function having a constant flank slope.

certain dielectric fit results (open symbols), α and *a* have parallel traces between 70 and 120 °C (α_1). The curved α trace part (α_2) starts near the bend temperature (≈70 °C). The α intensity (Figure 12b) shows some runout above 95 °C that can tentatively be interpreted by different intensities for two α processes, too: α_1 for higher temperatures with a higher onset temperature ($T_{on}(\alpha_1) \approx 130 \pm 5$ °C) and low $d\Delta\epsilon/d(1/T)$ slope, and α_2 with lower onset temperature ($T_{on}(\alpha_2) \approx 95 \pm 5$ °C) but a steeper intensity slope. Both onsets are indicated by circles in the Arrhenius diagram (inset of Figure 12a). Including α_1 (or not) has a large influence on the WLF parameters, of course. The different WLF traces are also indicated in the inset of Figure 12a. The parallelism between *a* and α for $T > 60$ °C cannot be modeled by any WLF function. All onset properties of both α's for the 38% S sample are also included in Figure 8a−c.

It is the high-temperature α_1 properties that fit well to the parameters of the samples with other styrene fractions. All of them are calculated with inclusion of all α values. The first indication of some runout is at the 19% S sample.

Although the α_1 intensity is weak, the indication for some peculiarity there can be seen by the naked eye in the original ϵ'' experimental points (Figure 13) as a bend in the low-frequency flank of the ϵ'' peak. Such a bend cannot be represented by a one-HN function fit.

In summary, parts a and b of Figure 12 show that the small cooperativity at the α onset is sensitive to molecular details: two molecular mechanisms for minimal cooperativity are perhaps possible near the α onset of the 38% S copolymer sample.

References and Notes

(1) Adam, G.; Gibbs, J. H. *J. Chem. Phys.* **1965**, *43* , 139.
(2) Donth, E. *J. Non-Cryst. Solids* **1982**, *53*, 325.
(3) Mohanty, U. *J. Chem. Phys.* **1994**, *100*, 5905.
(4) Ediger, M. D.; Angell, C. A.; Nagel, S. R. *J. Phys. Chem.* **1996**, *100*, 13200.
(5) 1st International Discussion Meeting on Relaxations in Complex Systems, Herakleon, Greece 1991. *J. Non-Cryst. Solids* **1992** , *131−133*.
(6) 2nd International Discussion Meeting on Relaxations in Complex Systems, Alicante, Spain 1994. *J. Non-Cryst. Solids* **1994** , *172−174*.
(7) Rössler, E. *Phys. Rev. Lett.* **1990**, *65*, 1595.
(8) Fischer, E. W. *Physica A* **1993**, *201*, 183.
(9) Donth, E. *Glasübergang;* Akademie: Berlin, 1981.
(10) Garwe, F.; Schönhals, A.; Lockwenz, H.; Beiner, M.; Schröter, K.; Donth, E. *Macromolecules* **1996**, *29*, 247.
(11) Zeeb, S.; Höring, S.; Garwe, F.; Beiner, M.; Hempel, E.; Schönhals, A.; Schröter, K.; Donth, E. *Polymer* **1997**, *38* , 4011.
(12) Vogel, H. *Phys. Z.* **1921,** *22*, 645. Fulcher, G. S. *J. Am. Ceram. Soc.* **1925,** *8*, 339. Tammann, G.; Hesse, G. *Z. Anorg. Allg. Chem.* **1926**, *156*, 245.
(13) Williams, M. L.; Landel, R. F.; Ferry, J. D. *J. Am. Chem. Soc.* **1955**, *77*, 3701.
(14) Domberger, W.; Reichert, D.; Garwe, F.; Schneider, H.; Donth, E. *J. Phys.: Condens. Matter* **1995**, *7*, 7419.
(15) Garwe, F.; Schönhals, A.; Beiner, M.; Schröter, K.; Donth, E. *J. Phys.: Condens. Matter* **1994**, *6*, 6941.
(16) Donth, E. *J. Polym. Sci. Part B: Polym. Phys. Ed.* **1996**, *34*, 2881.
(17) Kulik, A. S.; Radloff, D.; Spiess, H. W. *Macromolecules* **1994**, *27*, 3111.
(18) McCrum, N. G.; Read, B. E.; Williams, G. *Anelastic and dielectric effects in polymer solids*; John Wiley: London, 1967.
(19) Donth, E.; Kahle, S.; Korus, J.; Beiner, M. *J. Phys. I Fr.* **1997**, *7*, 581.
(20) see e.g. Roth, H.-K.; Keller, F.; Schneider, H. *HF-Spektroskopie in der Polymerforschung*; Akademie: Berlin, 1984.
(21) Press, W. H.; Flannery, B. P.; Teukolsky, S. A.; Vetterling, W. T. *Numerical Recipes in Pascal (Fortran, C). The Art of Scientific computing*; Cambridge Univ. Press: Cambridge, England/New York, 1992.
(22) Havriliak, S.; Negami, S. *J. Polym. Sci., Part C* **1966**, *14*, 99.
(23) Havriliak, S.; Negami, S. *Polymer* **1967**, *8*, 161.
(24) Mott, N. F.; Davis, R. A. *Electronic processes in non-crystalline materials*; Clarendon: Oxford, England, 1979.
(25) Böttcher, C. F.; Bordewijk, P. *Theory of electric polarization, Vol. 2: Dielectrics in time-dependent fields*; Elsevier: Amsterdam, 1978.
(26) Williams, G.; Watts, D. C. In *NMR Basic Principles and Progress*; Diel, P., Fluck, E., Kosfeld, R., Ed.s.; Springer: Berlin, 1971; Vol. 4.
(27) Alvarez, F.; Hoffman, A.; Alegria, A.; Colmenero, J. *J. Chem. Phys.* **1996**, *105*, 432.
(28) Arbe, A.; Richter, D.; Colmenero, J.; Farago, B. *Phys. Rev. E* **1996**, *54*, 3853.
(29) Korus, J.; Beiner, M.; Busse, K.; Kahle, S.; Donth, E. *Thermochim. Acta*, in press.
(30) Schröter, K.; Reissig, S.; Garwe, F.; Kahle, S.; Unger, R.; Beiner, M.; Donth, E. To be published.
(31) Beiner, M.; Korus, J.; Lockwenz, H.; Schröter, K.; Donth, E. *Macromolecules* **1996**, *29*, 5183.
(32) Donth, E.; Beiner, M.; Reissig, S.; Korus, J.; Garwe, F.; Vieweg, S.; Hempel, E.; Schröter, K. *Macromolecules* **1996**, *29*, 6589.
(33) Donth, E. *J. Phys. I Fr.* **1996**, *6*, 1189.
(34) Donth, E.; Korus, J.; Hempel, E.; Beiner, M. *Thermochim. Acta*, in press.
(35) Pschorn, U.; Rössler, E.; Sillescu, H.; Kaufmann, S.; Schaefer, D.; Spiess, H. W. *Macromolecules* **1991**, *24*, 398.
(36) Schneider, K.; Schönhals, A.; Donth, E. *Acta Polym.* **1981**, *32*, 471.
(37) Heijboer, J. In *Physics of Non-crystalline solids*; Prins, J. A., Ed.; North-Holland: Amsterdam, 1965; p 231.
(38) Debye, P. *Polare Molekeln*; Hirzel: Leipzig, Germany, 1929.
(39) Floudas, G.; Placke, P.; Stepanek, P.; Brown, W.; Fytas, G.; Ngai, K. L. *Macromolecules* **1995**, *28*, 6799.
(40) Beiner, M. Private communication.
(41) Reissig, S. Private communication.
(42) Pfandl, W.; Link, G.; Schwarzl, F. R. *Rheol. Acta* **1984**, *23*, 277. Plazek, D. J. *Polym. J.* **1980**, *12* , 43.
(43) Richter, D.; Farago, B.; Fetters, L. J.; Huang, J. S.; Ewen, B.; Lartigue, C. *Phys. Rev. Lett.* **1990**, *64*, 1389.
(44) Menon, N.; O'Brien, K. P.; Dixon, P. K.; Wu, L.; Nagel, S. R.; Williams, B. D.; Carini, J. P. *J. Non-Cryst. Solids* **1992**, *141*, 61.

MA961933B